Laboratory Investigation (2020) 100:1425–1435
https://doi.org/10.1038/s41374-020-0467-7

ARTICLE

The synthetic toxin biliatresone causes biliary atresia in mice

Yifan Yang[1] · Junfeng Wang[1] · Yong Zhan[1] · Gong Chen[1] · Zhen Shen[1] · Shan Zheng[1] · Rui Dong[1]

Received: 26 April 2020 / Revised: 24 June 2020 / Accepted: 24 June 2020 / Published online: 17 July 2020

Abstract

Exposure to environmental toxins may be responsible for biliary atresia. The focus of this study was to investigate the effect of biliatresone on the development of the hepatobiliary system in mice. We successfully synthesized biliatresone with a purity of 98% and confirmed its biliary toxicity. Exposure to high doses of biliatresone caused abortion or death in pregnant mice. Neonatal mice injected with biliatresone developed clinical signs of biliary obstruction, and dysplasia or the absence of extrahepatic biliary tract lumen, which confirmed the occurrence of biliary atresia. In the portal tract of biliary atresia mice, signs of infiltration of inflammatory cells and liver fibrosis were observed. The signature of extrahepatic biliary gene expression in these mice mainly involved the cell adhesion process, and hepatic RNA-seq was highly linked to transcriptional evidence of oxidative stress. When compared with the control group, hepatic glutathione levels were markedly reduced after biliatresone injection. Taken together, these data confirm that biliatresone causes severe developmental abnormalities of the hepatobiliary system in mice. Furthermore, decreased levels of glutathione may play a mechanistic role in the pathogenesis of liver fibrosis in biliatresone-induced experimental biliary atresia.

Introduction

Biliary atresia (BA) is a multifactorial liver disease that is characterized by inflammation and fibrosis of the extrahepatic biliary tract in infants. If left untreated, BA liver fibrosis will rapidly develop into end-stage liver cirrhosis [1]. The etiology of BA is still unknown, and evidence for genetic pathogenic hypothesis is limited [2–4]. An increased number of studies have focused on environmental factors, including viral infection and toxin exposure [5–7]. The proposed mechanism in the pathogenesis of BA involves a virus or toxin that causes an inflammatory reaction or autoimmune damage of bile duct epithelial cells, which finally leads to the occurrence of BA [8]. The Rhesus rotavirus (RRV)-induced BA mouse model has helped to better understand the essential role of immunity and inflammation in BA pathogenesis [9]. However, currently there is no conclusive evidence of viral infections in patients with BA [10, 11].

Recently, a natural uncharacterized toxin, biliatresone, was isolated from the Dysphania species that was implicated in outbreaks of BA in Australian livestock [12, 13]. Biliatresone is the first toxin known to cause selective destruction of the extrahepatic biliary tree in zebrafish larvae, which resemble the pathology observed in human BA. These findings indicate a potential link between toxin-induced biliary injury and human BA, and that exposure to certain environmental factors could be an important triggering event in BA. In this study, we synthesized biliatresone as described previously [14], and investigated the effect of biliatresone on development of the hepatobiliary system in mice.

Materials and methods

Synthesis of biliatresone and toxicity testing

Biliatresone was synthesized as described previously [14] with minor modifications (Supplementary Fig. 1) by SIMR

Supplementary information The online version of this article (https://doi.org/10.1038/s41374-020-0467-7) contains supplementary material, which is available to authorized users.

✉ Shan Zheng
szheng@shmu.edu.cn

✉ Rui Dong
rdong@fudan.edu.cn

[1] Department of Pediatric Surgery, Children's Hospital of Fudan University, Shanghai Key Laboratory of Birth Defect, and Key Laboratory of Neonatal Disease, Ministry of Health, 399 Wan Yuan Road, Shanghai 201102, China

Biotech., Ltd. (Shanghai, China). All zebrafish (wild-type, Tu) were raised in the Children's Hospital of Fudan University Zebrafish Facility in accordance with the protocols approved by the Institutional Animal Care and Use Committee of the Fudan University. Lyophilized biliatresone was resuspended in anhydrous DMSO and added to embryo media for zebrafish at final concentrations of 0.1 μg/ml, 0.15 μg/ml, and 0.2 μg/ml, containing 0.1% DMSO. Assays were repeated in triplicate with at least 30 larvae. After treatment for 48 h, biliary morphologies were evaluated in live larvae using Bodipy-C16 and 2F11 maker as previously described [13].

Experimental model of BA induced by biliatresone

Breeding pairs of Balb/c mice were kept in micro isolator cages in a virus-free environment. Mice had free access to sterilized chow and water. Animal studies were performed in accordance with protocols and regulations that were approved by the Institutional Animal Care and Use Committee at Children's Hospital of Fudan University. Various doses of biliatresone (10–50 μg/g of body weight) were administrated at different gestational days (day 4–18) to pregnant mice using a single or daily intraperitoneal injection. All doses were repeated in at least three pregnant mice. Pregnant mice were monitored for weight daily until delivery. Pups were monitored every other day for weight and jaundice.

Newborn mice of which the mothers were not administrated toxin, underwent intraperitoneal injection at 12 h–72 h after birth at a dosage of 30–100 μg biliatresone. Saline-injected pups served as controls. All doses were repeated in at least 30 pups. Pups were monitored every other day for weight, jaundice, and acholic stool. In addition, symptoms and survival rates were recorded. Pups were sacrificed at 14 days post injection, and livers and bile ducts were harvested for further analysis.

Histology and immunohistochemistry

At 14 days post injection, livers and extrahepatic bile ducts were harvested from mice that received biliatresone and saline. Livers were fixed in 10% formalin, embedded in paraffin, and sectioned at 5 μm along the length of the section. Next, sections were stained with hematoxylin and eosin (HE) and Masson-trichrome. Immunohistochemistry was performed as previously described [15]. Briefly, sections were heated in citrate buffer (pH 6.0) for 15 min after deparaffinization and rehydration. Subsequently, sections were incubated overnight at 4 °C with the following antibodies: anti-CK19 (Abcam, 1:400, ab52625), anti-CD8 (Abcam, 1:1000, ab209775), anti-CD4 (Abcam, 1:1000, ab183685), anti-F4/80 (Abcam, 1:100, ab111101), and an antibody against cellular tubulin (Invitrogen, 1:200, 62204). Sections were washed for 20 min in PBST, then incubated with a secondary antibody (GeneTech, Shanghai, China). Finally, sections were visualized by diaminobenzidine solution (GeneTech, Shanghai, China).

Measurement of serum ALT, AST, TB and MMP7, and tissue glutathione (GSH)

Levels of serum alanine aminotransferase (ALT), aspartate aminotransferase (AST), total bilirubin (TB) (Jiancheng, Nanjing, China), and matrix metalloproteinase 7 (MMP-7) (Cloud-clone, Wuhan, China) were measured in (1:20 PBS diluted) serum samples collected at 14 days post injection. Tissue GSH concentrations were determined with a Micro Reduced GSH Assay Kit (Solarbio, Beijing, China). All assays were performed following the manufacturer's recommendations.

RNA extraction and RT-qPCR

At 14 days after administration of saline or biliatresone, Balb/c pups were sacrificed, and their livers and extrahepatic bile ducts (including gallbladders and common bile ducts) were harvested. Total RNA was extracted from liver tissues using Trizol reagent (Invitrogen, Carlsbad, CA, USA) according to the manufacturer's guidelines. Next, Itga2, Serpine1, Thbs1, Ccl2, Mmp7, Cxcl2, Cxcl5, Cxcl1, Gclc, Gclm, Gsta3, and Gsto2 mRNA levels were determined using the SYBR green method; β-actin served as an internal reference as previously described [15]. Primer sequences are shown in Supplementary Table 1.

RNA sequencing and pathway analysis

Livers and extrahepatic bile ducts RNA were extracted from six biliatresone-treated BA mice and three controls, and sequencing was performed by Genergy Bio-Tech Corporation (Shanghai, China). To construct libraries for sequencing, the TruSeq RNA Library Prep Kit v2 for Illumina (San Diego, CA, USA) was used. Final libraries were quantified by the PicoGreen dsDNA Assay Kit (Invitrogen, Carlsbad, CA, USA). Next, libraries were sequenced on a Hiseq 2500 platform (Illumina, San Diego, CA, USA). Differentially expressed genes (DEGs) were assessed using Cuffdiff, with a false discovery rate (FDR) correction for multiple testing. DEGs were considered significant when $P \le 0.05$ and an intensity change (fold ≥ 2) between comparisons. DEGs were grouped and analyzed using Gene Ontology (GO) and KEGG (Kyoto Encyclopedia of Genes and Genomes) pathway enrichment analysis. All original sequence data were deposited in the NCBI's Sequence Read Archive database (SRA accession: PRJNA597175).

Statistical analyses

Statistical analyses were presented as the mean ± standard deviation using the Student's *t* test. Kaplan–Meier curves and barplots were generated using GraphPad Prism 8 (San Diego, CA, USA). $P < 0.05$ was considered statistically significant.

Results

Synthesized biliatresone caused BA in zebrafish

Using high-performance liquid chromatography, we successfully synthesized biliatresone with a purity of 98% (Supplementary Fig. 1). The toxicity of synthetic biliatresone was observed in zebrafish larvae at 5 days post-fertilization as described previously [13]. Extrahepatic bile ducts were easy to recognize in larvae that were treated with low doses of biliatresone (0.1 μg/ml), whereas larvae treated with higher doses (0.15 μg/mL) for 24 h only showed subtle gallbladder defects. Treatment with 0.15 μg/mL biliatresone for 48 h or 0.2 μg/mL biliatresone for 24 h resulted in pronounced morphological defects of zebrafish larvae gallbladder and extrahepatic ducts (Supplementary Fig. 2). Gallbladders were severely dysmorphic, and extrahepatic bile ducts were difficult to recognize, suggesting that the synthetic biliatresone had similar biliary toxic effects compared with natural biliatresone.

Biliatresone induced clinical manifestations of BA in neonatal mice

We used various doses of biliatresone (30–100 μg per mouse) at different days (12 h–72 h after birth) in multiple combinations, and identified that a dose of 80 μg at 24 h–48 h after birth resulted in a maximum number of mice exhibiting BA symptoms. Injection of biliatresone resulted in a high mortality (48.9%) within the first 7 days post injection (Fig. 1a),

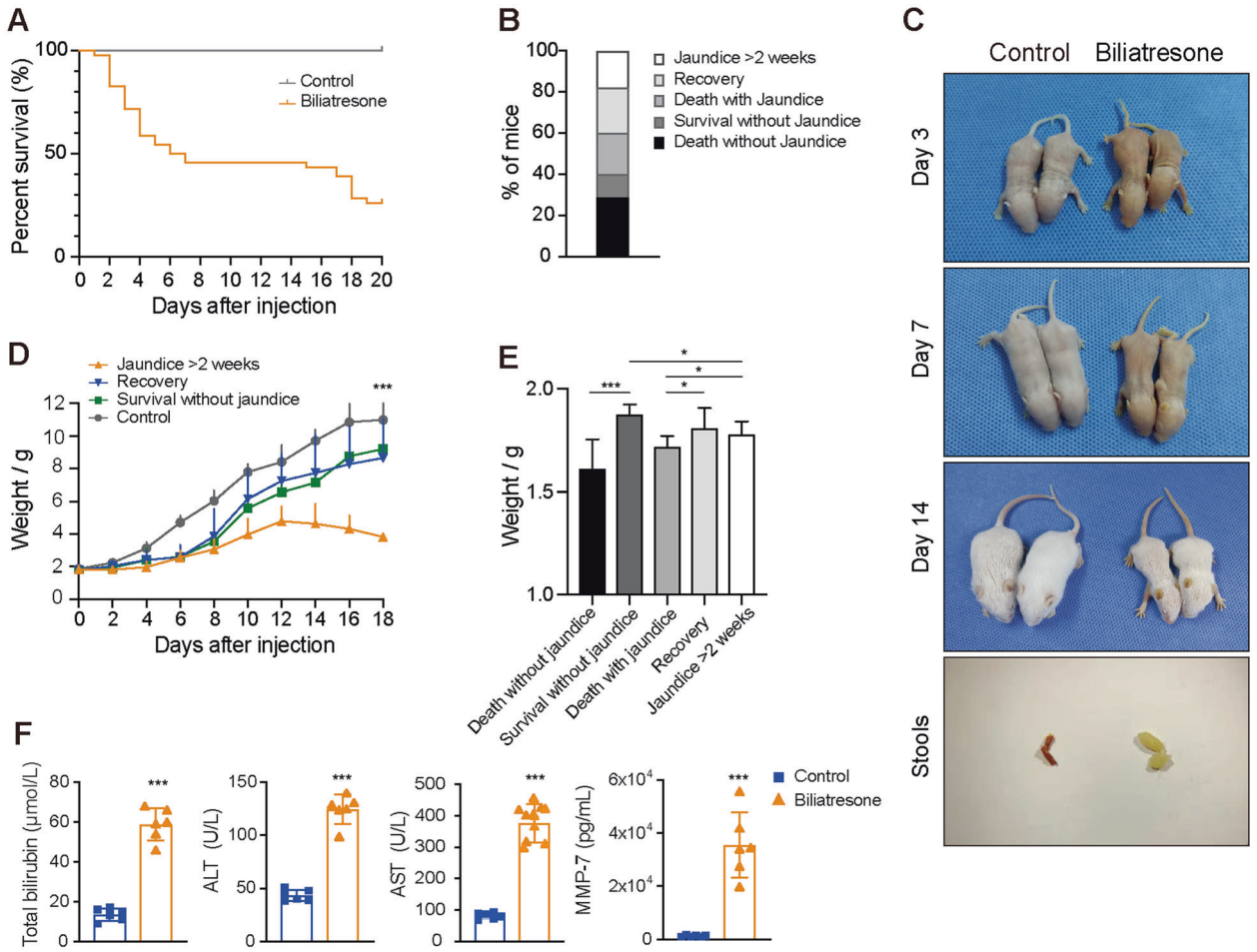

Fig. 1 Biliatresone induced clinical manifestations of BA in neonatal mice. Survival curve (**a**), jaundice rate (**b**), clinical signs of biliary obstruction (**c**), and development of weight (**d**) in mice after biliatresone and saline injection. The body weight of mice with different outcomes at injection (**e**). Serum levels of ALT, AST, TB, and MMP-7 were measured in mice with persistent jaundice and controls at 14 days post injection. $N = 90$ and 20 samples for the biliatresone and the saline injection group, respectively. *$p < 0.05$, **$p < 0.01$, ***$p < 0.001$.

including death with jaundice (20%) and without jaundice (28.9%, Fig. 1b). Moreover, no developmental abnormalities or jaundice were observed in 11.1% of the injected pups ("Survival without jaundice" group, Fig. 1b). Most of the injected mice developed cholestasis starting from day 2 to day 4 post injection. Jaundice in 17.8% of the injected pups could persist more than 2 weeks (Fig. 1b), with a maximum of 18 days until death. When compared with healthy controls, jaundiced pups with clinical signs of biliary obstruction showed bilirubinuria, acholic stools, and growth retardation (Fig. 1c, d). The greatest difference in weight between biliatresone-injected pups and saline controls was noted at day 18 post injection (3.82 ± 0.20 vs. 10.98 ± 0.70, respectively, Fig. 1d). However, some jaundiced pups (22.2%) recovered from the biliary toxicity by a weight gain and relief of clinical symptoms during the first 7 days after injection ("Recovery" group, Fig. 1b).

The weight at injection of mice with different outcomes were further investigated (Fig. 1e). We found that the body weight of both mice in the death without jaundice group (1.61 ± 0.14 g, $p < 0.01$) and in the death with jaundice group (1.72 ± 0.05 g, $p < 0.05$) was significantly lower compared with mice in the survival without jaundice group (1.88 ± 0.04 g), persistent jaundice group (1.78 ± 0.06 g), and the recovery group (1.81 ± 0.09 g). No significant differences were observed between the persistent jaundice group and the recovery group ($p = 0.458$).

Serum levels of ALT (124.7 ± 13.8 vs. 43.3 ± 5.2 U/L), AST (375.8 ± 61.2 vs. 79.83 ± 9.3 U/L), and TB (58.8 ± 8.1 vs. 13.5 ± 3.1 μmol/L) in mice with persistent jaundice were higher than that of controls, suggesting liver injury ($p < 0.001$, Fig. 1f). We further measured MMP-7 serum levels in mice. At 2 weeks post injection, markedly elevated serums levels of MMP-7 (35574.0 ± 12325.0 vs. 1273.0 ± 319.7 pg/mL, $p < 0.001$) were detected in mice with persistent jaundice (Fig. 1f).

Biliatresone caused developmental abnormalities of the hepatobiliary system in mice

Livers and extrahepatic bile ducts of mice were harvested at 14 days after treatment with biliatresone or saline. The gross morphology of the extrahepatic biliary tree revealed different patterns of injury (Fig. 2a). The gallbladders of pups

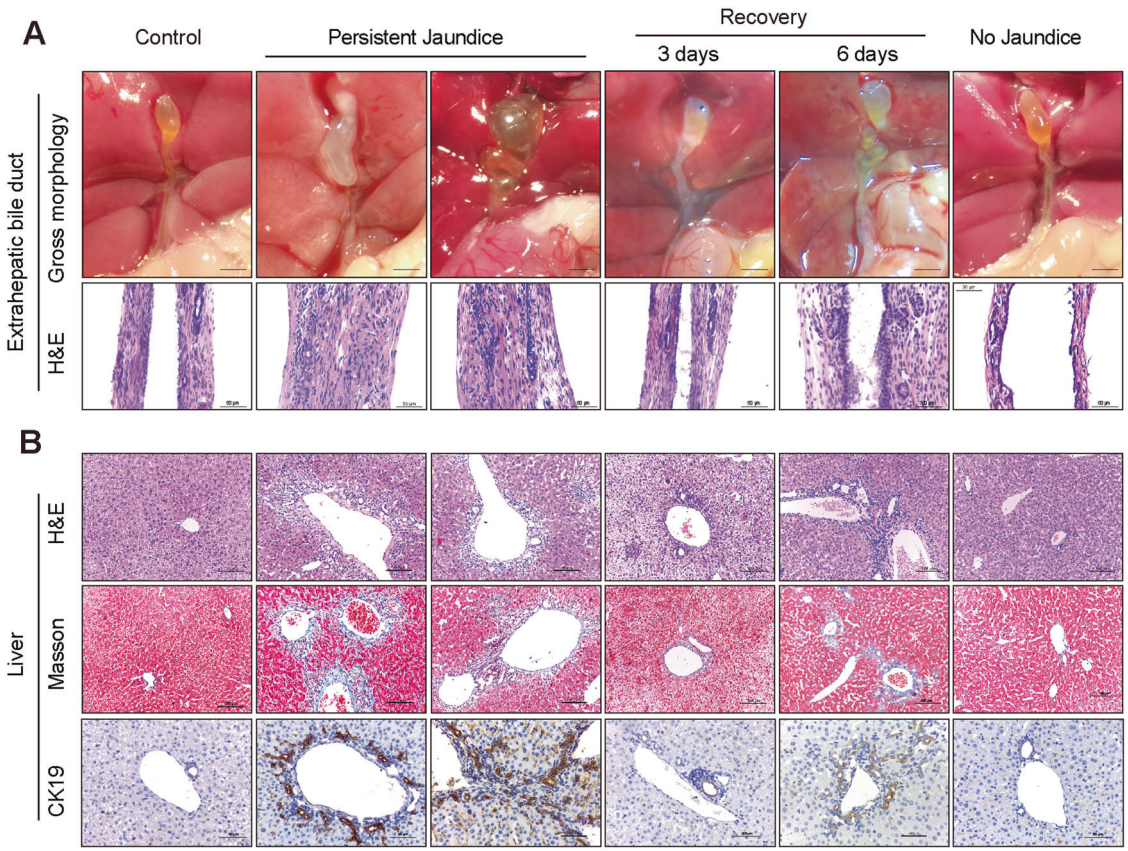

Fig. 2 Biliatresone caused developmental abnormalities of the hepatobiliary system in mice. Gross morphology and HE staining of extrahepatic biliary tree in mice with different outcomes at 14 days post injection (**a**). HE staining, Masson staining, and CK19 staining of the liver of mice with different outcomes at 14 days post injection (**b**). Scale bars: 2 mm for the gross morphology of extrahepatic biliary duct. 50 μm for HE staining of bile duct and CK19 staining. Scale bars: 100 μm for HE and Masson staining of liver.

with persistent jaundice were abnormally enlarged and contained thick, white, or green inspissated bile with sludge. In addition, the common bile ducts were severely dilated and curled or indistinguishable from mice injected with saline. In recovery pups, the extrahepatic bile ducts were slightly enlarged and twisted, and varied with the duration of transient jaundice (3 or 6 days), and the structure of the lumen of common bile duct could be distinguishable. The structure of the extrahepatic biliary tree in mice without jaundice was similar as in the controls.

Histological analysis of the extrahepatic biliary tract of injected mice revealed the following notable findings (Fig. 2a). A complete absence of lumen, infiltration of inflammatory cells, and fibroblastic proliferation were observed in extrahepatic bile ducts of mice with persistent jaundice, indicating that BA occurred. Histological evaluation of the hepatobiliary tree of recovery pups revealed minimal or mild intraepithelial inflammation or hyperplastic reactive epithelium, which was consistent with the findings observed by gross morphology. In contrast, the inflammatory reaction rarely extended into the lumen of the bile duct in mice without jaundice.

Histological evaluation of the liver of mice with persistent jaundice showed evident infiltration of inflammatory cells, and mild to severe fibrosis within the area of the portal tract (Fig. 2b), which mimicked human BA. The histology of the livers of mice without jaundice and with transient jaundice was similar to that of controls. As expected, the distribution of CK19-stained bile ducts was disordered, and small ductules showed an abnormal proliferation in the hepatic portal tract of mice with persistent jaundice, (Fig. 2b), thereby indicating that proliferation occurred with obstruction. CK19 positive staining area ratios were 3.2 ± 0.8%, 23.9 ± 9.3%, 4.3 ± 0.5%, 12.3 ± 5.8%, and 2.9 ± 1.1% in the control group, persistent jaundice group, recovery groups (3 days and 6 days), and no jaundice group, respectively. When compared with RRV-induced BA mouse model, no significant differences were observed in the degree of inflammation and liver fibrosis in the biliatresone group at 14 days after injection (Supplementary Fig. 3). Furthermore, we evaluated the histology of kidney tissue by HE and Masson staining (Supplementary Fig. 4). When compared with controls, no obvious abnormalities were observed in biliatresone-induced BA mice, except for only mild inflammatory cell infiltration (Supplementary Fig. 4).

The gallbladder of mice treated with biliatresone and stained with CK19 demonstrated proliferation of cholangiocytes, and were abnormally disordered, while monolayer disruption with lumen obstruction were observed in extrahepatic bile ducts when compared with the control. In addition, reduced staining of cellular tubulin (microtubules maker) for CK19 + biliary epithelial cells of the gallbladder was observed in biliatresone-induced BA mice (Fig. 3). However, no significant reduction in tubulin staining was observed in extrahepatic bile ducts and intrahepatic cholangiocytes between biliatresone and control groups (Fig. 3).

Activation of immune cells in livers of biliatresone-induced BA models

To preliminarily explore the potential cellular mechanisms in biliatresone-induced BA mice, we investigated the activation of hepatic macrophages, CD4+, and CD8+ T cells by immunohistochemistry (Fig. 4). In the liver parenchyma of mice injected with saline, immune cells were scattered sporadically. F4/80+ macrophages showed a diffuse distribution in fibrous septa, portal tracts, and parenchyma area in BA models, and the majority of CD4+ and CD8+ T cells were distributed in the portal tract, which was similar to BA patients as reported previously [16]. Taken together, these findings suggested a potential contributory role for the immune response in biliatresone-induced liver injury.

Extrahepatic biliary and hepatic gene expression signatures for biliatresone-induced mice of BA

We performed RNA-seq on six mice in the BA group and three control mice of which extrahepatic bile duct and liver tissues were harvested at 14 days. DEGs were selected based on statistical analysis (P value ≤ 0.05) and intensity change (fold ≥ 2). In total, we identified 1378 upregulated and 3150 downregulated genes in extrahepatic bile duct tissues of BA mice when compared with control mice. Moreover, KEGG and GO pathway enrichment analysis revealed that these DEGs were mainly related to neuroactive ligand−receptor interaction, cell adhesion molecules, retinol metabolism, chemical carcinogenesis, steroid hormone biosynthesis, complement and coagulation cascades, metabolism of xenobiotics by cytochrome p450, and cytokine−cytokine receptor interaction (Fig. 5). We observed a significant downregulation of genes involved in cell adhesion processes, including the claudin family (*Cldn1, Cldn5, Cldn8, Cldn10, Cldn14, Cldn20*), cadherin family (*Cdh2, Cdh4, Cdh5*), cell adhesion molecule 3, intercellular adhesion molecule 2, and junction adhesion molecule 2.

A total of 4329 DEGs with 2661 upregulated genes and 1668 downregulated genes were identified in liver tissues of BA mice. KEGG pathway analysis showed that these DEGs were involved in chemical carcinogenesis, retinol metabolism, peroxisome, metabolism of xenobiotics by cytochrome p450, cell adhesion molecules, the MAPK signaling pathway, glutathione metabolism, and butanoate metabolism (Fig. 6a). In addition, GO analysis demonstrated that

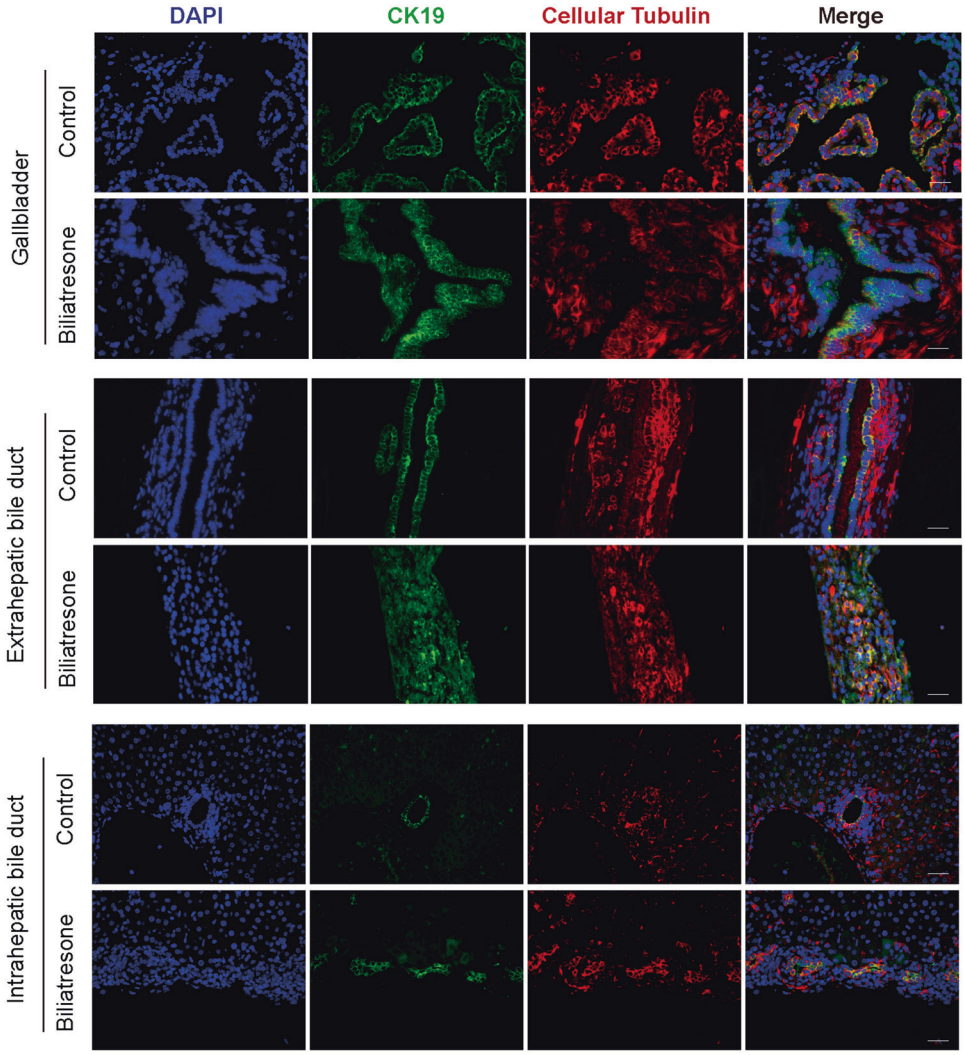

Fig. 3 Reduced staining of cellular tubulin for CK19+ biliary epithelial cells of the gallbladder in biliatresone-induced BA mice. The gallbladder, extrahepatic bile duct, and intrahepatic bile duct were stained for cellular tubulin (red) or CK19 (green) in biliatresone-induced BA models and controls at 14 days post injection. Nuclei were stained with DAPI (blue). Scale bars: 25 μm.

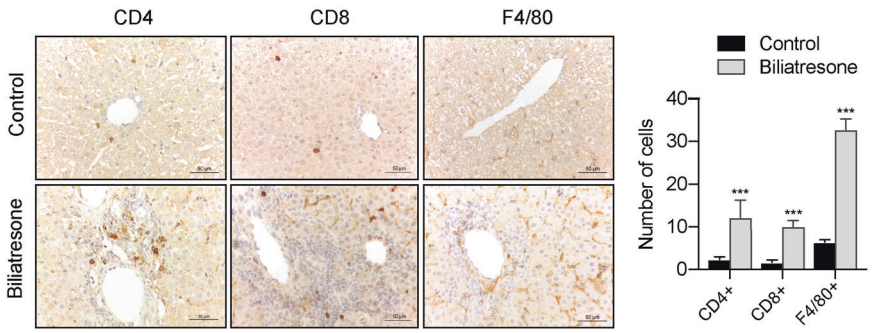

Fig. 4 Activation of immune cells in the liver of biliatresone-induced BA models. Distribution of CD4+ and CD8+ T cells, and F4/80+ macrophages in the liver of biliatresone-induced BA models and controls at 14 days post injection. Scale bars: 50 μm. ***$p < 0.001$.

DEGs associated with response to wounding, oxidation-reduction processes, and inflammatory responses in the biological process category, catalytic activity, and oxidoreductase activity in the molecular function category were significantly enriched (Fig. 6b).

Of the 15 unique overexpressed genes identified in human BA as described previously [17], 12 genes were significantly upregulated in the liver of biliatresone-induced BA mice as based on the RNA-seq results (Fig. 6c), including *Vcan, Ccl20, Vtcn1, Itga2, Serpine1, Thbs1, Ccl2, Lamc2, Areg, Slc2a3, Mmp7, Cxcl1, Cxcl2*, and *Cxcl5* (representing the murine homologu of human IL8). The mRNA expression levels of individual genes were detected. The expression of *Itga2, Serpine1, Thbs1, Ccl2, Mmp7,*

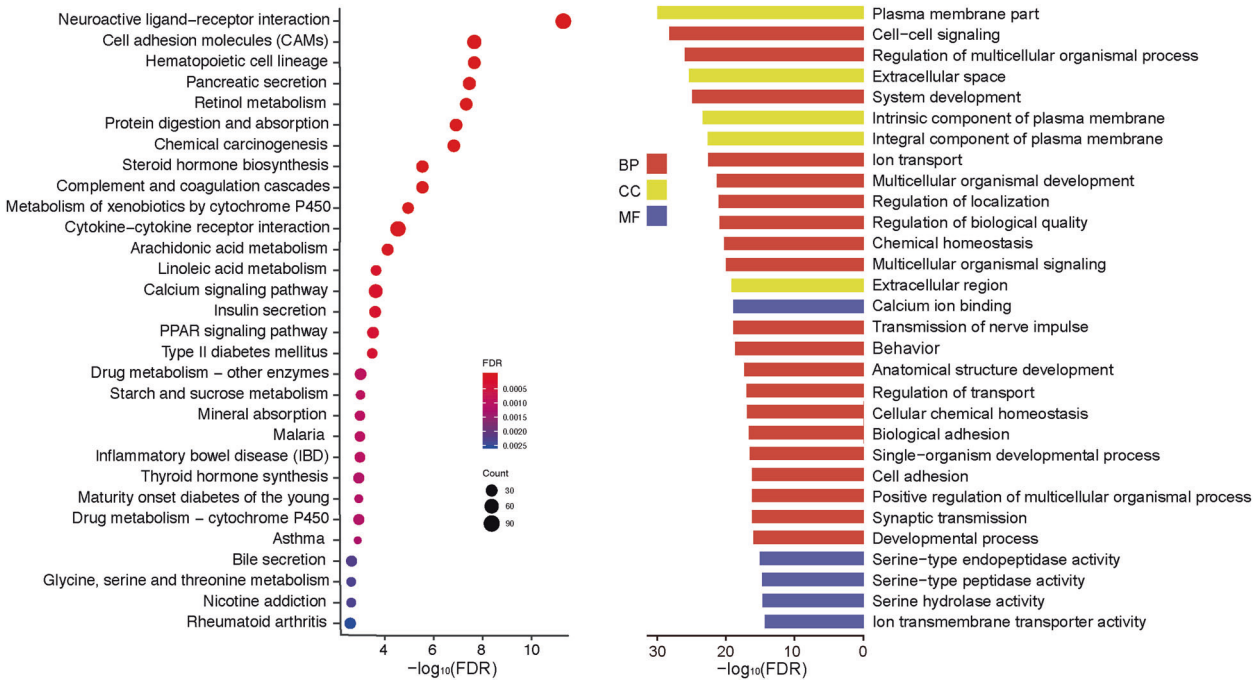

Fig. 5 Extrahepatic biliary gene expression signature for the biliatresone-induced mouse model of BA at 14 days post injection. The dot plot (left) depicted the top 30 most significant KEGG pathways that were enriched in differentially expressed genes by RNA-seq in livers of BA and control mice. The histogram (right) represented the top 30 most significant biological processes (BP), cell components (CC) and molecular function (MF) by Gene Ontology (GO) enrichment analysis of differentially expressed genes. FDR false discovery rate.

Cxcl2, and *Cxcl5*, but not *Cxcl1*, increased 1.5–5-fold above the controls in the liver at 14 days after injection (Fig. 6d).

Hepatic GSH depletion in biliatresone-induced BA mice

The GO analysis of DEGs showed that the oxidation-reduction activity may play a prominent role in biological processes and molecular function. Moreover, the GSH metabolism pathway showed the highest statistical significance to the oxidation-reduction process based on KEGG pathway analysis. In a previous study, the importance of GSH in modulating biliatresone-induced hepatobiliary system injury in zebrafish was revealed [18]. Therefore, we further investigated the expression of GSH metabolism-related genes in the liver of biliatresone-induced BA mice.

As shown in the heat map of GSH metabolism-related genes from hepatic DEGs mentioned above (Fig. 6e), a significant downregulation of genes involved in the encoding for enzymes required for GSH biosynthesis was observed (glutamate-cysteine ligase [gclc]) and metabolism (glutathione S-transferase [gsto2, gsta3, gstt1, gstk1, gstm4]). Supporting this, we also observed significant downregulation of gclm, gclc, gsto2, and gsta3 by RT-qPCR (Fig. 6f). Compared with the control group, the GSH level in the liver was reduced nearly fivefold after biliatresone-injection (Fig. 6f). GSH levels in matched kidney samples showed no significant changes between biliatresone and control groups at day 14 (data not shown).

High-dose biliatresone caused abortion or death in pregnant mice

Various doses of biliatresone (10–50 μg/g body weight) were used in pregnant mice at different gestational days (day 4–18) using a single or daily intraperitoneal injection. Death occurred within 2 days after injection with 50 μg/g biliatresone. Excessive bleeding from the vagina of dead mice and no obvious abnormalities in parenchymal organs after dissection were found, however the cause of bleeding was unknown. Several pregnant mice (days 4, 6, 8, 10, 12, 14, and 16 of pregnancy), that were once injected with 30 or 40 μg/g biliatresone, gradually lost weight to the pre-pregnancy level, indicating abortion. Other mice showed a short-term decrease in weight, then slowly gained weight until delivery, and the number of births dropped significantly. No developmental abnormalities or jaundice were observed in these pups within 14 days after birth. Daily injection of low doses (10 or 20 μg/g) of biliatresone to pregnant mice (from day4, 6, 8, and 10 of pregnancy) resulted in only 2 to 4 births per maternal mice. No jaundice or hepatobiliary dysplasia were found within 14 days after birth.

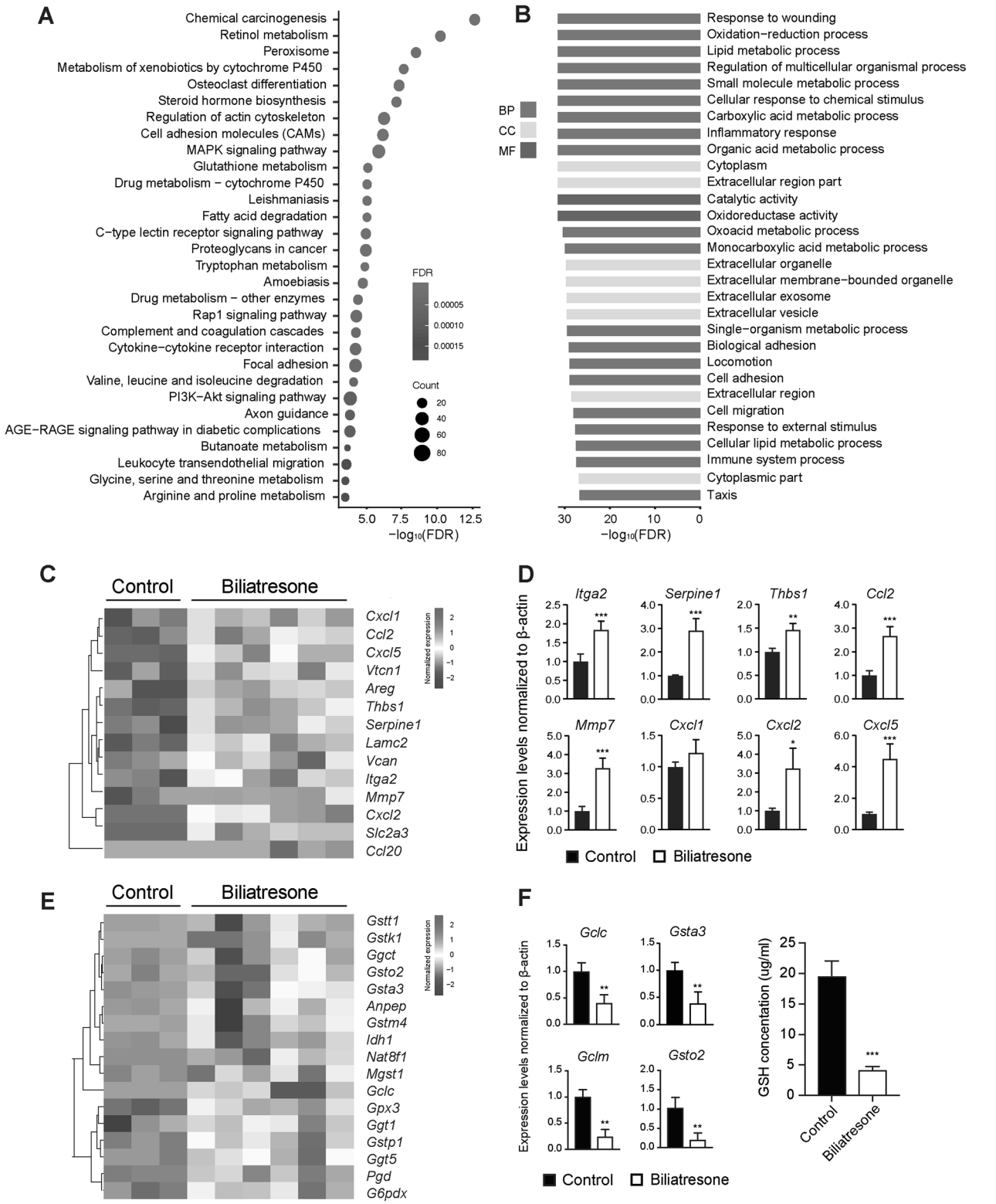

Fig. 6 Hepatic gene expression signature for the biliatresone-induced mouse model of BA at 14 days post injection. KEGG pathway (**a**) and GO enrichment analysis (**b**) of differentially expressed genes (DEGs) by RNA-seq in the liver of BA and control mice. Heat map of the over-expression of Vcan, Ccl20, Vtcn1, Itga2, Serpine1, Thbs1, Ccl2, Lamc2, Areg, Slc2a3, Mmp7, and Cxcl1, Cxcl2, and Cxcl5 from hepatic DEGs (**c**). mRNA expression of Itga2, Serpine1, Thbs1, Ccl2, Mmp7, Cxcl2 Cxcl5, and Cxcl1 in the liver of BA and control mice (**d**). Heat map of the expression of GSH metabolism-related genes from hepatic DEGs (**e**). mRNA expression of gclm, gclc, gsto2, gsta3 by RT-qPCR. Levels of hepatic GSH in BA and control mice at 14 days post injection (**f**). $^{**}p < 0.01$, $^{***}p < 0.001$. BP biological process, CC cellular component, MF molecular function.

Discussion

Identification of biliatresone suggested that exposure to environmental toxins could be responsible for BA, therefore, the focus of this study was to investigate the effect of biliatresone on the development of the hepatobiliary system in mice. We synthesized biliatresone as described previously with minor modifications. Zebrafish larvae treated with synthetic biliatresone had morphological defects of the gallbladder and extrahepatic ducts as described before, however, the dose of biliatresone (0.2 μg/ml 48 h) was less than reported in the previous study (0.5 μg/ml 48 h) [13]. These data suggested that synthetic biliatresone had the same biliary toxic effect compared with natural biliatresone, indicating it could be used in future mammal studies.

Reports of a natural BA outbreak showed that affected animals grazed the Dysphania species in the early stages of pregnancy [12]. Hepatoblasts differentiated into cholangiocytes on embryonic day 14.5 (E14.5), and primitive bile ducts or tubules start to form at E16.5 in mice [19, 20]. Thus, we chose mice at 8, 12, 14, and 16 days of pregnancy by two different administration ways (intraperitoneal injection and intragastric gavage) using 50 μg/g of body weight biliatresone. Most mice that received an intraperitoneal injection died or lost weight to the pre-pregnancy level, whereas all mice that underwent intragastric gavage steadily gained weight up to delivery. No jaundice was observed in newborn pups within 14 days. These findings indicated that the effect of intraperitoneal injection of biliatresone on pregnant mice was most evident, which could greatly reduced the dosage of biliatresone and was more convenient. Hence, for all subsequent studies, intraperitoneal injection was used. Various doses of biliatresone (10–50 μg/g of body weight) induced different outcomes on pregnant mice, including death, miscarriage, and reduced litter size. However, newborn mice did not show symptoms of cholestasis, which might be related to the biliatresone dosage and treatment we used or associated with species differences. In the flock of congenital BA outbreaks, only sheep and cattle of mixed breeds were affected [12].

We intraperitoneally injected various doses of biliatresone (30–100 μg each) at 12 h–72 h after birth once or repeatedly. Jaundice was observed in several groups, and most jaundiced mice either died, or recovered from the cholestasis symptoms within 7 days post injection. Only mice in two groups (80 μg, 24 h–48 h, once and 60 μg, 24 h–48 h, twice) developed persistent jaundice more than 2 weeks, but did not survive longer than 3 weeks, which was similar to the natural BA livestock [12]. The persistent jaundice rate (17.8% vs. 12.8%) was higher in the 80 μg group with a lower mortality rate (48.9% vs. 57.4%) compared with the 60 μg group. Considering the high mortality and recovery rate, we compared the weight at the time of injection to identify the ratio of biliatresone dose to mouse weight. The results showed that the weight of dead mice was lower than survival mice that received the same dose. In addition, no significant differences in body weight were observed between recovery and persistent jaundice mice. The cause of recovery from jaundice was unknown. However, the weight of recovery mice was still slower than controls.

Serum levels of MMP7 demonstrated good accuracy in diagnosing BA from other neonatal cholestasis with alternative causes [21], which was further confirmed by our recent large-cohort study [22]. Serum levels of MMP-7 were measured in our mouse model. The concentration of MMP-7 was nearly 30-fold higher in the persistent jaundice group, which was similar to the levels found in human BA. Gross morphology and histology of the extrahepatic biliary tree confirmed the clinical manifestations. The gallbladders of pups injected with biliatresone were abnormally enlarged and contained thick inspissated bile because of obstruction of the distal bile duct. Instead of biliary epithelial cell lining, infiltrated inflammatory cells and stromal proliferation were observed in obstructed bile ducts tissue of mice with persistent jaundice, which was consistently observed in the RRV model and BA epidemic in livestock [12, 23]. The proliferation of cholangiocytes was induced by cholestasis and biliary obstruction, and the activation of biliary proliferation was thought to play a key role in the initiation and progression of liver fibrosis [24, 25]. Jaundiced mice showed markedly increased expression of CK19-positive bile ducts in portal tracts, which could be a significant pathological feature of BA. In a previous study, it was demonstrated that the cellular infiltration in the portal tract in BA livers at diagnosis represented a CD4+ Th1 cell-mediated inflammatory processes [16]. We showed a similar result, and found extensive infiltration of CD4+ and CD8+ T cells as well as Kupffer cells in the portal tracts of the biliatresone model at 14 days after injection. Decreased tubulin staining of extrahepatic biliary epithelial cells, but not intrahepatic cholangiocytes, reflected destabilization or depolymerization of microtubules in biliatresone-induced BA mice. The results also confirmed selective extrahepatic biliary toxicity of biliatresone.

To identify extrahepatic bile duct and liver-specific expressed genes, we analyzed the transcriptome by RNA-seq from BA mice and controls. DEGs in extrahepatic bile duct were linked to an abundance of downregulated cell adhesion-related genes, including the claudin family, cadherin family, cell adhesion molecules, and junction adhesion molecules. This supports the finding that biliatresone increased cholangiocyte monolayer permeability [26], however, these findings still need to be validated at the post-transcriptional level. Hepatic gene expression signatures indicated that a total of 4329 DEGs were highly enriched in

response to wounding, oxidation-reduction processes, inflammatory responses, cell adhesion molecules, the MAPK signaling pathway, and glutathione metabolism, and these results had a substantial overlap in biological processes or pathways in BA patients. Numerous transcriptomic investigations showed that a molecular signature of BA has potential implications for the diagnosis and development of biomarkers [15, 17, 27]. In a large cohort study, 15 unique genes were identified that formed a signature with high sensitivity and specificity in BA patients, especially IL8 and LAMC2 [17]. Our RNA-seq results showed that 12 genes were significantly upregulated in the liver of biliatresone-induced BA mice, which may be relevant to the pathogenesis of liver injury in the experimental model.

Among the GO enrichment analysis and pathways with the highest statistical significance, two pathways were related to the oxidation-reduction process and one was enriched for glutathione metabolism. These findings implied a transcriptional response to oxidative stress. Excessive or uncontrolled production of oxidative radicals can cause damage to nucleic acids, proteins, and lipids, which were closely associated with human liver disease pathogenesis [28, 29]. GSH is the most abundant cellular antioxidant, and the level of regulation of GSH homeostasis is provided by GCL (composed by the GCLC and GCLM subunit) and GST, along with other antioxidant enzymes that protect the cell against oxidative damage [29]. By further analyzing the glutathione gene signature, we found that GSH metabolism-related genes (gclm, gclc, gsto2, gsta3) as well as the GSH content decreased in the liver of biliatresone-induced BA mice, which was consistent with hepatic GSH depletion in zebrafish that were treated with biliatresone [18]. Furthermore, no significant reduction in GSH level was observed by co-treatment with a high dose of N-acetyl-cysteine (a GSH precursor) when compared with larvae that were treated with biliatresone alone [18]. In other animal studies, it was also shown that hepatic expression of the GSH synthetic gene decreased markedly along with GSH levels at later stages of bile duct ligation (BDL) mice, and a lower hepatic GSH content greatly potentiated BDL-induced liver fibrosis [30, 31]. In contrast, preventing the reduction in hepatic GSH resulted in amelioration of hepatic fibrosis [32]. Taken together, these findings raised the possibility that effective antioxidative stress may alleviate hepatic injury and enhance improved survival in BA.

In conclusion, our study showed that biliatresone could cause severe developmental abnormalities of the hepatobiliary system in neonatal mice, which were similar to human BA in both pathology and molecular signature. Redox stress signaling could be important for mediating the toxic damage response of biliatresone, and decreased levels of GSH may play a mechanistic role in the pathogenesis of liver fibrosis in biliatresone-induced experimental BA.

Acknowledgements This study received financial support from Shanghai Key Disciplines (no. 2017ZZ02022), Shanghai Municipal Key Clinical Specialty (no. shslczdzk05703), National Natural Science Foundation of China (no. 81770519, no. 81771633, no. 81873545 and no. 81974059), The Science Foundation of Shanghai (no. 18411969100 and no. 19ZR1406600), and Children's National Medical Center (no. EK1125180104, no. EKYY20180204, EK112520180211 and no. EK112520180310).

Compliance with ethical standards

Conflict of interest The authors declare that they have no conflict of interest.

Publisher's note Springer Nature remains neutral with regard to jurisdictional claims in published maps and institutional affiliations.

References

1. Davenport M. Biliary atresia: clinical aspects. Semin Pediatr Surg. 2012;21:175–84.
2. Garcia-Barceló MM, Yeung MY, Miao XP, Tang CS, Cheng G, So MT, et al. Genome-wide association study identifies a susceptibility locus for biliary atresia on 10q24.2. Hum Mole Genet. 2010;19:2917–25.
3. Leyva-Vega M, Gerfen J, Thiel BD, Jurkiewicz D, Rand EB, Pawlowska J, et al. Genomic alterations in biliary atresia suggest region of potential disease susceptibility in 2q37.3. Am J Med Genet A. 2010;152A:886–95.
4. Rurarz M, Czubkowski P, Chrzanowska K, Cielecka-Kuszyk J, Marczak A, Kamińska D, et al. Biliary atresia in children with aberrations involving chromosome 11q. J Pediatr Gastroenterol Nutr. 2014;58:e26–e29.
5. Riepenhoff-Talty M, Schaekel K, Clark HF, Mueller W, Uhnoo I, Rossi T, et al. Group a rotaviruses produce extrahepatic biliary obstruction in orally inoculated newborn mice. Pediatr Res. 1993;33:394–9.
6. Mack C. The pathogenesis of biliary atresia: evidence for a virus-induced autoimmune disease. Semin Liver Dis. 2007;27:233–42.
7. Tyler KL, Sokol RJ, Oberhaus SM, Le M, Karrer FM, Narkewicz MR, et al. Detection of reovirus RNA in hepatobiliary tissues from patients with extrahepatic biliary atresia and choledochal cysts. Hepatology. 1998;27:1475–82.
8. Petersen C, Davenport M. Aetiology of biliary atresia: what is actually known? Orphanet J Rare Dis. 2013;8:128.
9. Petersen C. Biliary atresia: the animal models. Semin Pediatr Surg. 2012;21:185–91.
10. Rauschenfels S, Krassmann M, Al-Masri AN, Verhagen W, Leonhardt J, Kuebler JF, et al. Incidence of hepatotropic viruses in biliary atresia. Eur J Pediatr. 2009;168:469–76.
11. Mack CL, Feldman AG, Sokol RJ. Clues to the etiology of bile duct injury in biliary atresia. Semin Liver Dis. 2012;32:307–16.
12. Harper P, Plant JW, Ungers DB. Congenital biliary atresia and jaundice in lambs and calves. Aust Vet J. 1990;67:18–22.
13. Lorent K, Gong W, Koo KA, Waisbourd-Zinman O, Karjoo S, Zhao X, et al. Identification of a plant isoflavonoid that causes biliary atresia. Sci Transl Med. 2015;7:286ra67.
14. Estrada MA, Zhao X, Lorent K, Kriegermeier A, Nagao SA, Berritt S, et al. Synthesis and structure–activity relationship study

of biliatresone, a plant isoflavonoid that causes biliary atresia. ACS Med Chem Lett. 2018;9:61–4.
15. Dong R, Yang Y, Shen Z, Zheng C, Jin Z, Huang Y, et al. Forkhead box A3 attenuated the progression of fibrosis in a rat model of biliary atresia. Cell Death Dis. 2017;8:e2719.
16. Mack CL, Tucker RM, Sokol RJ, Karrer FM, Kotzin BL, Whitington PF, et al. Biliary atresia is associated with cd4+ th1 cell–mediated portal tract inflammation. Pediatr Res. 2004;56:79–87.
17. Bessho K, Mourya R, Shivakumar P, Walters S, Magee JC, Rao M, et al. Gene expression signature for biliary atresia and a role for Interleukin-8 in pathogenesis of experimental disease. Hepatology. 2014;60:211–23.
18. Zhao X, Lorent K, Benjamin JW, Marchione DM, Gillespie K, Waisbourd-Zinman O, et al. Glutathione antioxidant pathway activity and reserve determine toxicity and specificity of the biliary toxin biliatresone in zebrafish. Hepatology. 2016;64:894–907.
19. Zong Y, Stanger BZ. Molecular mechanisms of liver and bile duct development. Wiley Interdiscip Rev Dev Biol. 2012;1:643–55.
20. Li Z, White P, Tuteja G, Rubins N, Sackett S, Kaestner KH. Foxa1 and Foxa2 regulate bile duct development in mice. J Clin invest. 2009;119:1537–45.
21. Lertudomphonwanit C, Mourya R, Fei L, Zhang Y, Gutta S, Yang L, et al. Large-scale proteomics identifies MMP-7 as a sentinel of epithelial injury and of biliary atresia. Sci Transl Med. 2017;9:eaan8462.
22. Jiang J, Wang J, Shen Z, Lu X, Chen G, Huang Y, et al. Serum mmp-7 in the diagnosis of biliary atresia. Pediatrics. 2019;144:e20190902.
23. Allen SR, Jafri M, Donnelly B, McNeal M, Witte D, Bezerra J, et al. Effect of rotavirus strain on the murine model of biliary atresia. J Virol. 2007;81:1671–9.
24. Glaser SS, Gaudio E, Miller T, Miller T, Alvaro D, Alpini G. Cholangiocyte proliferation and liver fibrosis. Expert Rev Mol Med. 2009;11:e7.
25. Lichtman SN, Sartor RB. Duct proliferation following biliary obstruction in the rat. Gastroenterology. 1991;100:1785–7.
26. Waisbourd-Zinman O, Koh H, Tsai S, Lavrut P-M, Dang C, Zhao X, et al. The toxin biliatresone causes mouse extrahepatic cholangiocyte damage and fibrosis through decreased glutathione and SOX17. Hepatology. 2016;64:880–93.
27. Luo ZH, Shivakumar P, Mourya R, Gutta S, Bezerra JA. Gene expression signatures associated with survival times of pediatric patients with biliary atresia identify potential therapeutic agents. Gastroenterology. 2019;157:1138–52.
28. Ye ZW, Zhang J, Townsend DM, Tew KD. Oxidative stress, redox regulation and diseases of cellular differentiation. Biochim Biophys Acta. 2015;1850:1607–21.
29. Lu SC. Glutathione synthesis. Biochim Biophys Acta. 2013;1830:3143–53.
30. Yang H, Ramani K, Xia M, Ko KS, Li TW, Oh P, et al. Dysregulation of glutathione synthesis during cholestasis in mice: Molecular mechanisms and therapeutic implications. Hepatology. 2009;49:1982–91.
31. Ramani K, Tomasi ML, Yang H, Ko K, Lu SC. Mechanism and significance of changes in glutamate-cysteine ligase expression during hepatic fibrogenesis. J Biol Chem. 2012;287:36341–55.
32. Yang H, Ko K, Xia M, Li TW, Oh P, Li J, et al. Induction of avian musculoaponeurotic fibrosarcoma proteins by toxic bile acid inhibits expression of GSH synthetic enzymes and contributes to cholestatic liver injury in mice. Hepatology. 2010;51:1291–301.